Thermodynamic Prediction of Calcium Aluminate Cement Paste

Lapyote Prasittisopin[*1], *Arkom Boonpunya*[2] *and Issara Sereewatthanawut*[3]
[1, 2, 3] *Faculty of Engineering and Technology, Pathumthani University, Thailand*
**Corresponding author: lapyote@gmail.com*

Abstract

Calcium Aluminate Cement (CAC) is widely used in civil engineering application for some time. Research per thermodynamic prediction shows that the dissolution and nucleation behaviors reflect the ion concentration of the CAC system in solution. This study presents a theoretical prediction of calcium and aluminate ion concentrations of CAC system on dissolution and nucleation behavior, induction time (t_{ind}), interfacial free energy (**γ**), and crystal growth mechanism. Such data can influence the early-age hydration of CAC. Better understanding of the data is applied to predict and manipulate its early-age hydration. It is well understood that at 20°C the CAC compositions of $CaAl_2O_4{\cdot}10H_2O$ (CAH_{10}) and $Ca_2Al_2O_5{\cdot}8H_2O$ (C_2AH_2) were the main hydrated products. Results in the study indicated that the nucleation of calcium phase was the controlling nucleation mechanism, not the aluminate.

Keyword: Calcium Aluminate Cement, Dissolution, Ion concentration

Introduction

A core goal of modern material physics is the control of its interfaces and polymorph down to the atomic scale. Particularly, thermodynamic behaviors of metastable materials strongly depend on atomic-scale structural roughness, surrounding temperature, and chemical additive added. Hydraulic cement, an inorganic binder, is being hydrated with water and can convert into metastable phase. The conversion of metastable phase occurs in various cement types and in particular on Calcium Aluminate Cement (CAC). A selective means on controlling nucleation and growth mechanisms of such metastable phase can govern performance characteristics of resulting product and drives toward more sustainable and more efficient process.

Received: 17 October 2019
Revised: 6 November 2019
Accepted: 22 December 2019
Online publication date: 7 January 2020

CAC can be used in many applications such as refractory, rapid hardening, repairing, aerospace, and ceramic industries. It offers several advantages comparing to traditional portland cement system. These benefits include (1) reduced CO_2 emissions during manufacturing, (2) rapid strength gain, (3) high abrasion resistance, (4) high resistance to acid attack, (5) high dimensional stability, and (6) high thermal resistance (Scrivener KL. and *et al*., ,1998)

Early-age hydration behavior of most cementitious systems can affect both early- and later-age performance of the hydrated product. (Prasittisopin L. and *et al*., 2018; Prasittisopin L. and *et al*., 2015; Prasittisopin L. and et al., 2015). For CAC hydration at early ages, its mechanisms typically begin with the ion dissolution of unhydrated CAC powder into solution. As unhydrated CAC powder is introduced with water, calcium and aluminate ions (the main ions in chemical composition of CAC) first release into solution. The calcium and aluminate ions then react with water molecule forming new compounds of $Ca(OH)_{2(aq)}$ and $Al(OH)_{3(aq)}$ (De Aza AH. and *et al*., 2003). Concentrations of both compounds rapidly increase and reach a supersaturated stage. After reaching the maximum supersaturation level, nucleation and precipitation mechanisms of $Ca(OH)_{2(aq)}$ and $Al(OH)_{3(aq)}$ compounds initiate nuclei and then precipitate into a new crystalline product. During precipitating, ion concentrations begin to drop. The precipitation and dissolution mechanisms continue forming the new hydrated products and eventually the ion concentration values are reaching close to equilibrium values. The hydration reaction stops when there is no void left for the new hydrated products, pore solution is all depleted, or the new products formed separate the unhydrated CAC grain from the pore solution. The CAC hydration mechanisms follow dissolution-crystallization steps though solution model and can be used to measure a dymanic reaction kinetics, based on Le Chatelier's principle. Its hydration process of ion is shown in Figure 1

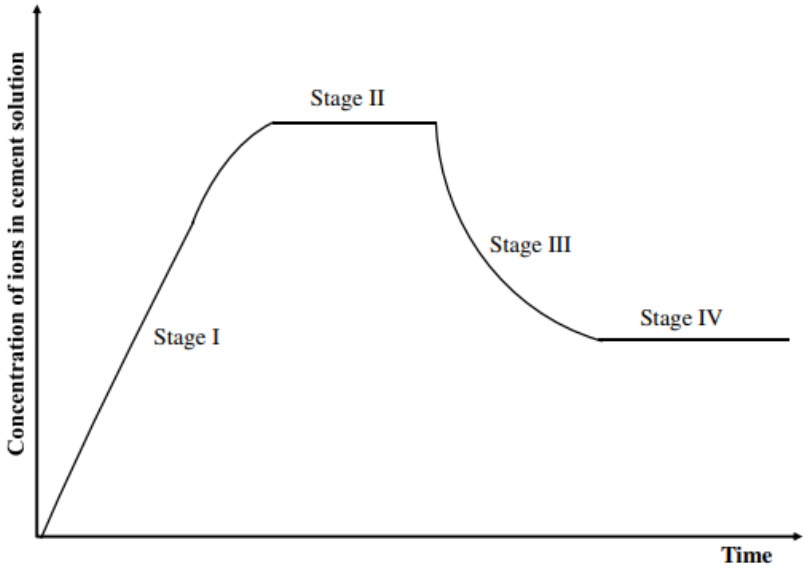

Figure 1. Hydration process of ions in cement systems: dissolution (Stage I), nucleation (Stage II), precipitation (Stage III), and continuous dissolution/precipitation (Stage IV).

Typical hydration reactions of CAC at 20°C are described as follows:[1]

- $CA + 10H_2O \rightarrow 2CAH_{10}$
- $2CA + 11H \rightarrow C_2AH_8 + AH_3$
- $2CAH_{10} \rightarrow C_2AH_8 + AH_3 + 9H$

(Cement nomenclature: C = CaO, A = Al_2O_3, H = H_2O, S = SiO_2, F = Fe_2O_3, Mg = MgO, Ti = TiO_2)

It is known that crystal structures of $CaAl_2O_4 \cdot 10H_2O$ (CAH_{10}) and $Ca_2Al_2O_5 \cdot 8H_2O$ (C_2AH_8) generally form as fine-needle- or rosette-like crystal and hexagonal crystal, respectively. When the hydration occurs at lower temperatures (between 15 and 30°C), both CAH_{10} and C_2AH_8 phases preferentially form (Scrivener KL. and *et al*., 1999). Another phase that can be formed at this temperature range is $Al(OH)_3$, which is an amorphous gel-like material. The amorphous $Al(OH)_3$ is reported to gradually crystallize to gibbsite with time (Prasittisopin L. and et al., 2015). According to the Ostwald's law, an initial phase reportedly formed during precipitation is the least stable, that is, the amorphous $Al(OH)_3$. However, gibbsite is the most thermodynamically equilibrium phase of the $Al(OH)_3$ systems (Bensted J. and *et al*., 2002; Price GJ. and *et al*., 2010; Ostwald W. and *et al*., 1990; Threlfall T. and *et al*., 2003) Therefore, all $Al(OH)_3$ is eventually transforming to gibbsite.

One analytical technique used to assess ion concentrations in solution is Atomic Absorption Spectroscopy (AAS). A benefit of using the AAS to measure ion concentration is that the concentrations are evaluated simultaneously. Compared with Inductively Coupled Plasma (ICP) technique, the AAS can in situ measure the ion concentration inexpensively over long time during hydration. The use of acid digestion or microwave digestion for storing

the solution and measure only one time is not precise because using strong acid to digest an alumina-rich material leads to a formation of a new complex compound and the acid may not able to dissolve all of the crystalline structure (Totten GE. and *et al*., 2003).

Research Objective

Although CAC has been implemented in many applications for a long time, the dissolution, nucleation, and precipitation mechanisms of the early-age hydration are not well explained. More scientific findings of these mechanisms enhance in-depth knowledge particularly on thermodynamic aspect affecting early-age hydration of CAC such that its performance of resulting products can be in the sense of better prediction and/or manipulation. The in-depth knowledge during early-age hydration of calcium and aluminate ions can be used to predict the t_{ind} and setting behavior of cementitious system. (Prasittisopin L. and *et al*., 2018; Prasittisopin L. and *et al*., 2015) Calcium and aluminate ion concentrations of CAC solution were in situ measured in this study. The measured ion concentration data are plotted on a binary calcium-aluminate solubility diagram of hydrating CAC system to identify the formation of hydrating products (Rodger SA and *et al*., 1984).

Experimental Sections

Materials

Unhydrated CAC (Secar 71) was procured from Kerneos (Chesapeake, VA) and was used in this research. Its X-Ray Diffraction (XRD) patterns were obtained by a Miniflex II diffractometer (Rigaku, The Woodlands, TX) with Cu Kα radiation and a graphite monochromator tested at 2° per min as shown in Figure 2. The XRD patterns show the main constituents of the CAC are $CaAl_2O4$ (CA) and $CaAl_4O_7$ (CA2). From Table 1, XRD analysis confirmed the major crystalline phase to be monocalcium aluminate (CA, ICDD file no. 23-1036), with grossite (CA_2, ICDD file no. 46- 1475), corundum (A, ICDD file no. 42- 1468), and diaoyudaoite ($NaAl_{11}O_{17}$, ICDD file no. 21- 1096) also present as secondary phases. Its chemical composition was analyzed by X-Ray Fluorescence and identified that: A = 68.5%, C = 31%, S < 0.8%, F < 0.4%, Ti < 0.4%, Mg < 0.5%, SO_3 < 0.3% and $K_2O + Na_2O$ < 0.5% and Blaine fineness is 3700 to 4500 cm^2/g. It is noted that the total composition of C and A equals 99.5% so the CAC in this study is considered as a dual-phase material with only minor impurities contained.

Table 1. XRD chemical composition of CAC.

XRD Chemical composition (%)			
Monocalcium aluminate	Grossite	Corundum	Diaoyudaoite
58.65	32.57	8.78	0.00

Water with the resistivity at 18.3 mΩ-cm purified by a Nano Pure II system was used throughout the experiment. Acetone (ACS grade; 99.5 wt%) and ethanol (ACS grade; 99.98 wt%) were used for removing moisture in order to stop hydration of the hydrating CAC for XRD and SEM studies

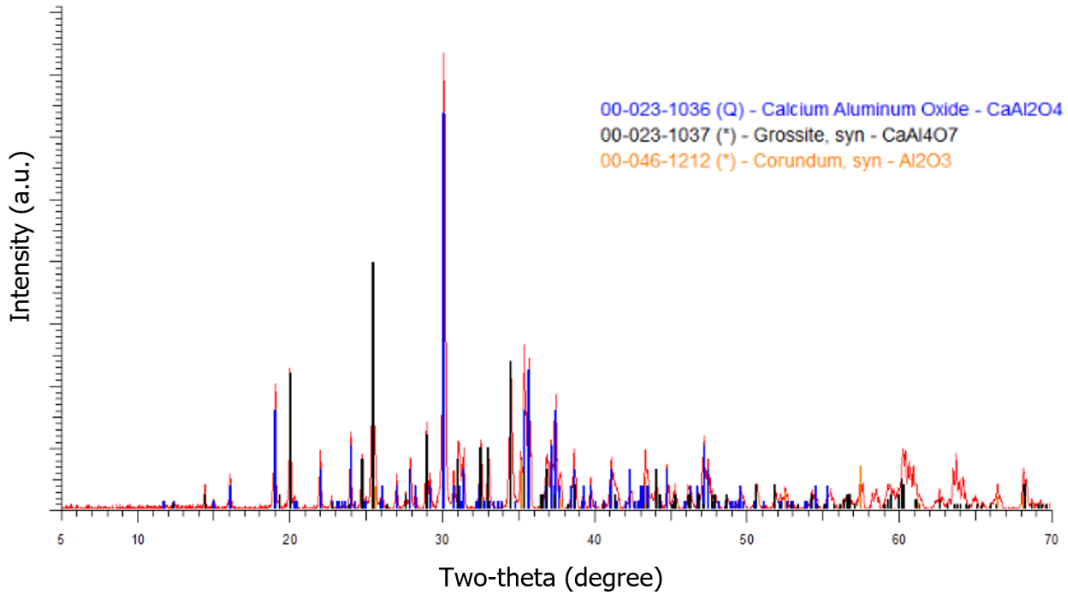

Figure 2. XRD pattern of unhydrated CAC powder.

Experimental Equipment and Procedures

An equipment setup and procedure for the measurement of t_{ind} in this present work was modified from the previous studies and illustrated in Figure 3. 21-23 Unhydrated CAC was mixed with water at a weight ratio between water and cement (w/c) value of 1.5. Previous studies reported that the w/c value of 1.5 exhibited no significant effect on the formation of resulting products and the w/c values ranging from 1.44 to 2.88 insignificantly affected the hydration kinetics in supersaturated solution. (Prasittisopin L. and *et al*., 2018; Prasittisopin L and *et al*., 2017; Parr C. and *et al*., 2008). Mixing was performed by using a magnetic stirrer (Corning, Lowell, MA) at 400 rpm and at the controlled temperature of 20 ± 2°C. The CAC paste was decanted from the mixing beaker and filtered using Whatman No. 40 filter paper. The filtrated solution used for measuring calcium ion concentration was diluted 100X in order to reduce the concentration down to an acceptable range that can be detected by AAS. The diluted solution was added 10 vol% of mixed lanthanum acid solution (50 g/l La_2O_3 in 3M HCl). The addition of the lanthanum acid solution promotes the reduction of interferences attributed by other elements (such as aluminate, silicate, and sodium) because the sensitivity of the detection of ions can be reduced in the presence of these elements.25 The sampling and preparation time of solution took up the first 3

minutes of the hydration time. Tested calcium ion solution at recorded hydration time was immediately determined by AAnalyst 100 AAS (Perkin Elmer Instrument, Waltham, MA) using air-acetylene gas at the wavelength of 422.7 nm. The hydration time represents the elapsed time after CAC powder is introduced with water until its ion concentration is detected by AAS. Calcium ion concentration was measured using AAS with nitrous oxide acetylene gas at the wavelength of 309.3 nm. Tested aluminate ion solution was diluted 10X allowing the concentration stays within the acceptable range. Each sample was measured the concentration values for three times and three samples were assessed for each condition. All mean values of total nine samples were reported here. An error bar represents a standard deviation of the nine samples calculated.

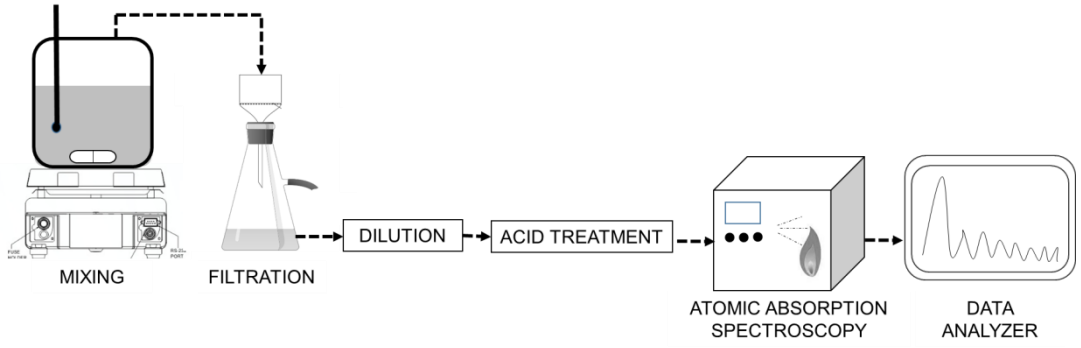

Figure 3. Experimental setup of t_{ind} measurement.

Results and Discussion

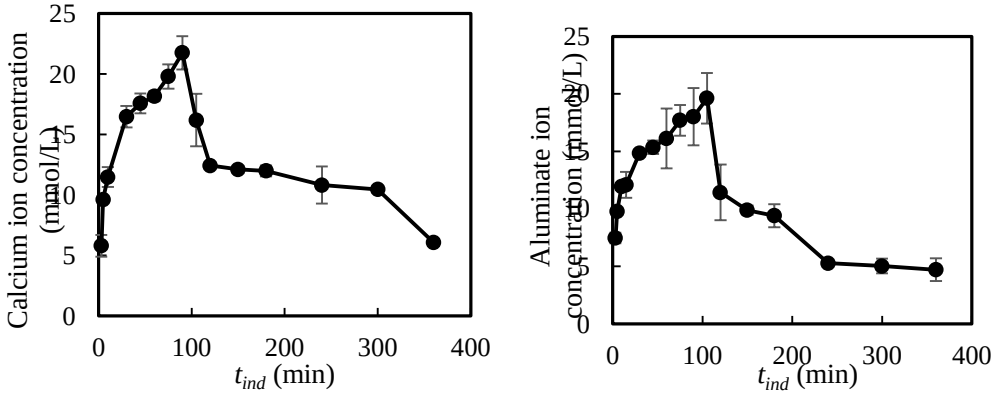

Figure 4. Relationship between t_{ind} and ion concentration of (a) calcium and (b) aluminate of hydrating CAC paste.

Figures 4a and 4b show the plots of ion concentration of calcium and aluminate ions of CAC paste versus the t_{ind}, respectively. The plots indicate that there is a good agreement between the experimental data and theoretical principle of hydration process of ions shown

in Figure 1. Figure 5 shows the binary solubility diagram of calcium-aluminate phases cured at 20°C, plotted on orthogonal axes. Points A, B, and C represent invariant points at 20°C. The invariant point is a unique condition of temperature, pressure, and concentration in the liquid system, resulting in a number of phases to coexist in equilibrium stage, based on Gibbs phase rule. (Smith JM and *et al*., 2000). For the binary diagram, two phases (calcium and aluminate) exist in the hydrating CAC system. Point A is the invariant point of the AH_3, CAH_{10}, and water. Point B is the invariant point of the CAH_{10}, C_2AH_8, and water. Point C is the invariant point of the C_2AH_8, $Ca_4AlO_7{\cdot}13H_2O$ (C_4AH_{13}), and water. These points (A, B, and C) were obtained from several empirical experiments from Jones (Jones FE. and *et al*., 1960) and Brown (Brown PW. and *et al*., 1986). A "tie line" is the line of particular hydrated product at a constant pressure and temperature condition representing a phase composition beyond the solubility limit. Its slope is calculated by the ratio between calcium and aluminate (C/A) for each hydrated phase.

The C/A values of 0, 1, 0.5, and 0.25 represent AH_2, CAH_{10}, C_2AH_8, and C_4AH_{13} phases, respectively. Transparent regions in Figure 4 represent the supersaturated boundaries of two phase regions (neighboring two solid phases). In these regions, the hydrating products precipitate either one or two phases. Grey-shaded regions represent supersaturated boundaries of one phase regions. In these regions, only single hydrated product precipitates. Each data on the diagram corresponds with the mean ion concentration value in CAC paste at the specified hydration time.

The fastest hydration time carried out in this work was measured at 3 minutes. Results indicate that the ion concentrations reach supersaturated stage only within the first few minutes after introducing water to the unhydrated sample. The region of the dash lines from 3 to 90 minutes associates with the dissolution stage of calcium and aluminate ions. The calcium ion concentration reaches 6 mmol/L at 3 minutes and reaches its maximum value of 21 mmol/L at 90 minutes. After 90 minutes, referred to as the line plotted on the CAH_{10} and AH_3 regions, the CAH_{10} begins to nucleate and grow in the supersaturated stage. As the growth mechanism of CAH_{10} continues, the calcium ion concentration decreases rapidly. It should be noted that the aluminate ion concentration during 90 to 105 minutes still increases from 18 mmol/L to the maximum level of 19 mmol/L although CAH_{10} have already precipitated. Hence, the mechanisms of dissolution and nucleation of aluminate ions is seemingly not a controlling mechanism of the precipitation of CAC.

During 240 to 300 minutes, the "outliners" of the paste composition are present, where the line representing on the region associates with the precipitation of the CAH_{10} and C_2AH_8. Meaningly, the predominant CAH_{10} phase precipitates as well as some of the C_2AH_8 precipitates. At the hydration time of 360 minutes, the main precipitating product is CAH_{10}. After this time, CAC paste begins stiffening and its temperature begins to increase

dramatically. Because the temperature increase affects the phase formation, the experiment is discontinued.

An arrow in Figure 5 can be interpreted as a "*time effect*" of the ion concentration of the calcium and aluminate systems of CAC paste cured at 20°C. Meaningly, a change of the ion concentration value as a function of hydration time or kinetics of ion concentration during the early-hydration. As mentioned earlier, the increase of ion concentration value can be referred to as the dissolution stage (Stage I in Figure 1); following by the decrease of ion concentration value that can referred to as the precipitation stage (Stage III in Figure 1). It is noted that the nucleation stage (Stage II in Figure 1) is disregarded because this stage cannot be measured by considering the time effect of the ion concentration. In Figure 5, since the calcium phase, as aforementioned, seems to control the hydration mechanism during this time period of 0 to 360 minutes. As calculated, the kinetics of dissolution and precipitation stages of CAC pastes equal approximately 0.23 and 0.06 mmol/L/min, respectively. The kinetics of the ion concentration differences of both stages at the hydration process ranging from 0 to 360 minutes indicate that the ion dissolution kinetics of CAC paste is about 4 times higher than the precipitation kinetics of CAC product. In respect of the Le Chatelier's principle, it is sound that the rate of dissolution is faster since much molecule of unhydrated CAC (reactant) presents in system, allowing that chemical equilibrium is under stress and consequently the chemical reaction shifts rapidly to reduce the stress.

Results of the binary calcium-aluminate solubility diagram indicate that the main composition of resulting products are CAH_{10} and AH_3. Partial quantity of hydrated C_2AH_8 product can also be found during early-age hydration. The calcium and aluminate ion concentrations rapidly increase in the dissolution stage and eventually drop to the equilibrium level when the precipitation mechanism is in progress.

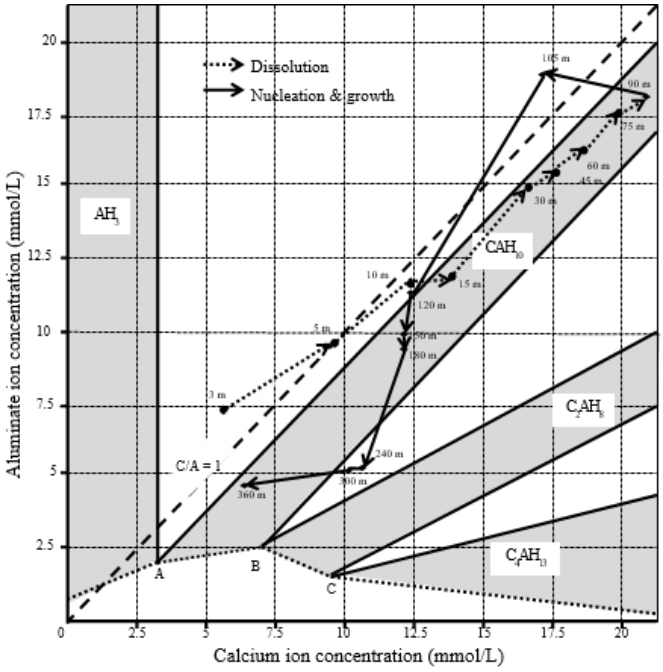

Figure 5. Binary solubility diagram of hydrating CAC paste cured at 20°C at the t_{ind} from 3 to 360 minutes (m = minutes of t_{ind}).

Conclusion

The current work presents the assessment and theoretical prediction of early-age hydration and growth mechanism of CAC system. The CAC is assumed to be binary system since the impurity is small. The conclusions of the work of the early-age hydration of CAC paste cured at 20°C can be drawn. The binary calcium-aluminate solubility diagram can be used to predict (1) the period of dissolution, nucleation, and precipitation taking place; (2) the phase controlling the precipitation mechanism; (3) the hydrating products forming, and (4) dynamic reaction kinetics of dissolution and precipitation. The results of the present work offer the scientific insight of using the principle of thermodynamic to assess the early-age hydration and growth mechanism of CAC and these are eventually used to better predict and/or manipulate the performance characteristics and durability of the hydrated product.

Reference

Bensted J. (2002). **In Structure and performance of cements**; 2nd ed.; In: Bensted J, Barnes P, editors. New York (US): Spon Press.

Brown PW. (1986). In: Proceedings of the 8th International Conference on the Chemistry of Cements; **Rio de Janeiro (Brazil).** Vol. 3, p 231.

De Aza AH, Pena P, Rodriguez MA, et al. (2003). **New spinel-containing refractory cements**. Eur Ceram Soc; 23(5):737–744.

Jones FE. (1960). **In: Proceedings of the 4th International Symposium on Chemistry of Cement;** 1960 Oct 2–7; Washington D.C: U.S. Department of Commerce. National Bureau of Standard.Vol. 1.

Ostwald W. (1990). **Zeitschrift für physikalische Chemie**. 34:495–503.

Price GJ, Mahon MF, Shannon J, et al. (2010). **Composition of calcium carbonate polymorphs precipitated using ultrasound.** Crys Growth Des. 11(1):39–44.

Prasittisopin L, Sereewatthanawut I. (2018). Effects of seeding nucleation agent on geopolymerization process of fly-ash geopolymer. **Front Struc Civil Eng**. 12(1):16–25.

Prasittisopin L, Trejo D. (2015). **Hydration and phase formation of blended cementitious systems incorporating chemically transformed rice husk ash**. Cem. Concr. Comp; 59:100–106.

Prasittisopin L, Trejo D. (2017). **Performance characteristics of blended cementitious systems incorporating chemically transformed rice husk Ash**. Adv Civil Eng Mater. 6(1):17–35.

Parr C, Fryda H, Liyama M, et al. (2008). Interractions of calcium aluminate cements and other matrixcomponents which control the initial hardening of deflocculated castables. **Technical paper**. TP-GB-RE-LAF-067. Kerneos; p.1-11.

Prasittisopin L, Trejo D. (2015). **Effects of mixing variables on hardened characteristics of portland cement mortars**. ACI Mater J ;112(3):399–407.

Rodger SA, Double DD. (1984). **The chemistry of hydration of high alumina cement in the presence of accelerating and retarding admixtures**. Cem Con Res. 14(1):73–82.

Scrivener KL, Capmas A. (1998). **Lea's chemistry of cement and concrete**. 4th ed. In: Hewlett PC, editor. New York (US): John Wiley & Sons.

Smith JM, Van Ness HC, (2000). **Abbott M. Introduction to chemical engineering thermodynamics**. 6th ed. McGraw-Hill.

Scrivener KL, Cabiron JL, Letourneux R. (1999). **Performance concretes from calcium aluminate cements**. Cem Con Res; 29:1215–1223.

Threlfall T. (2003). **Structural and thermodynamic explanations of Ostwald's rule**. Org Proc Res Dev; 7(6):1017–1027.

Totten GE, (2003). **MacKenzie DS. Handbook of aluminum: alloy production and materials manufacturing**. New York (US): Marcel Dekker AG.